actuators

MDPI

Article

A Two-Finger Gripper Actuated by Shape Memory Alloy for Applications in Automation Technology with Minimized Installation Space

Tobias Schmelter *, Lukas Bade and Bernd Kuhlenkötter

Chair of Production Systems, Ruhr-University of Bochum, Universitaetsstrasse 150, 44801 Bochum, Germany
* Correspondence: schmelter@lps.rub.de

Abstract: The increasing demand for innovative grippers and actuators for the automation sector encourages the development of new and innovative functional principles. Intelligent materials are particularly suitable for this purpose based on their high energy density. In this study, a two-finger gripper driven by shape memory alloys (SMA) for use in automation technology is presented. Previous grippers driven by SMA can only be found in the field of micro gripping due to the limited stroke generated by SMA. Based on a methodical product development, a new type of gripper was developed and is presented in this study, which can achieve an opening width comparable to conventional grippers based on transmission mechanisms. Two different variants of the gripper are shown and compared aiming to minimize the installation space and weight of the gripper. In addition to the design presentation, a prototype is built, and the functionality is demonstrated through various test series.

Keywords: shape memory alloys; shape memory actuator; actuator; automation technology; gripper

Citation: Schmelter, T.; Bade, L.; Kuhlenkötter, B. A Two-Finger Gripper Actuated by Shape Memory Alloy for Applications in Automation Technology with Minimized Installation Space. *Actuators* **2024**, *13*, 425. https://doi.org/10.3390/act13100425

Academic Editor: Manfred Kohl

Received: 21 August 2024
Revised: 13 October 2024
Accepted: 17 October 2024
Published: 21 October 2024

1. Introduction

Due to the increasing demands on performance, weight reduction, space savings, and reduced complexity for economical use in industry, grippers must always meet new requirements in the field of automation technology. New fields of application are continually being discovered, particularly in the field of aerospace technology, such as drones for transportation, as well as in the domain of miniaturization. Regarding sustainability, energy efficiency is also at the forefront of production, whereby technologies such as hydraulics and pneumatics are disadvantageous. New technologies such as shape memory alloys (SMA) are constantly used to develop new and better (smaller, lightweight, more energy efficient, etc.) actuators. SMA have the unique capability of autonomously returning to their original trained shape after a seemingly permanent plastic deformation. Through thermal activation, SMA autonomously returns to their original shape. This effect is often used for actuators in the form of SMA wires that contract, generating a stroke and force, to replace actuators, such as electric motors.

A gripper for automation technology, driven by SMA, enables a small installation space, low weight, and is controlled in a completely electrically and energy efficient way. Due to the high energy density of SMA compared to conventional actuators, a significant amount of work can still be accomplished. In traditional automation, the reduction in size and weight lowers the inertia at the end effector, enabling higher speeds and energy efficiency. Moreover, advanced automation systems, such as transport drones, require lightweight and compact grippers. Grippers powered by electric motors are typically heavy, which diminishes both the range and payload capacity of drones, while pneumatic and hydraulic systems are generally unsuitable for these applications [1].

This paper presents a new concept for an innovative two-finger gripper that achieves a large opening width of up to 40 mm and yet has a very low weight of just over 100 g.

SMA actuators found in the literature are either microgrippers with small opening widths of a few mm or are heavy and large when having larger opening widths (see Table 1). It was developed based on VDI 2248 [2–4] together with the design methods of Pahl/Beitz [5] up to a prototype. A primary objective is to minimize the installation space of the gripper while achieving a wide opening range through mechanical transmission.

2. Fundamentals

The following sections present the basics of SMA and gripper technologies. Furthermore, a brief overview of the state of the art in the field of grippers driven by SMA is given.

2.1. Shape Memory Alloys

The term "shape memory effect" (SME) refers to the ability of a material to return to a predefined shape after an apparent plastic deformation. This effect is induced by thermal or mechanical activation. Materials exhibiting this effect are known as shape memory alloys (SMA) [6,7]. Their main advantages include high energy density, low space requirements, control by internal sensor effect, and low weight [8]. The SME is based on a diffusionless phase transformation between the metallurgical structures martensite (low-temperature phase) and austenite (high-temperature phase) [9,10]. Based on the desired properties of the material, different effects can be imparted to the material through the alloy composition and thermomechanical training in the manufacturing process [6]. These are divided into pseudoelastic and pseudoplastic processes. The pseudoplastic processes can be further subdivided into the one-way effect and the two-way effect [11]. Different alloys exhibit the SME [6,12,13], the alloy that is used most frequently and economically in the field of actuators is a nickel titanium (NiTi) [2,14,15] alloy in which the mechanical two-way effect is thermally activated. The activation is achieved by applying an electrical voltage, which generates Joule heat, induction, or an ambient medium with an elevated temperature. This allows elongations of up to 8 % to be achieved by the phase transformation, with the recovery during the cooling of the material being generated by a counterforce in the form of a spring or an attached weight [6,8,11,16].

The SME is activated by an external impulse in the form of thermal energy. This thermal energy can be introduced by the environment or by an electrical current flow, which is converted into Joule heat based on the internal resistance of the material [17,18]. If the material is deformed and then heated, the microstructure is transformed from martensite to austenite starting at the austenite start temperature, A_S. Reaching the austenite finish temperature, A_F, the transformation process is completed, and the microstructure is exclusively austenitic. During this structural transformation, the atoms adopt the most energetically favorable arrangement, corresponding to the previously trained initial form. When the material cools down, the microstructure transforms again starting at the martensite start temperature, M_S, and when the martensite finish temperature, M_F, is reached, the microstructure is completely transformed again. During the austenite–martensite transformation, no further deformation takes place. This effect is referred to as the one-way shape memory effect (OWSME). The reverse deformation is generated by a constant counterforce in the form of an attached weight, antagonistic design, or spring. This generates a reverse deformation, leading to what is known as the extrinsic-induced two-way shape memory effect (TWSME) [13,19,20]. Figure 1 shows the relationship between the different structural states as a function of temperature and load for commercially available binary NiTi alloys, which are present in the unstressed state in the martensitic structure at room temperature. At the beginning of the process, a twinned martensite is present, which is de-twinned by an external mechanical stress resulting in the deformation of the material at the macroscopic level [6]. When the temperature surpasses the austenite start temperature during the heating process, the material undergoes a memory recall of its initial configuration. Upon reaching temperatures beyond the austenite finish temperature, the process of shape reversion achieves completion [21,22].

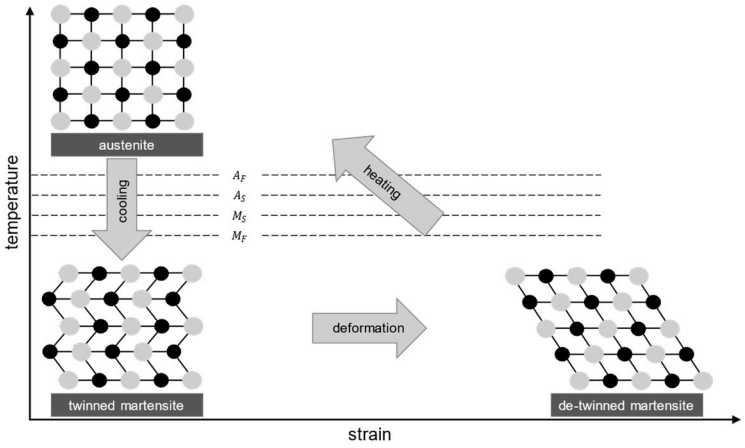

Figure 1. Representation of the thermal SME with the associated transformation temperatures and the lattice structure of NiTi.

During the martensite–austenite transformation, a stroke is generated by the change in the shape of the material. A force can also be generated by tensioning the material [7].

2.2. Gripper Technology

The following is an outline of the general structure of a gripper as it is used in the automation industry. Grippers can be divided into different categories based on the physical principle of operation: mechanical grippers, suction grippers, magnetic grippers, adhesion grippers, and needle grippers [23]. The main tasks of the gripper system can be divided into three categories: establishing contact between the gripper and the object (temporal force or shape pair connection), manipulating the object (change in position, rotation, or mounting), and setting down the gripped object (releasing the contact). Through these tasks, the gripper forms the link between the automation technology and the gripped object [24,25].

Figure 2 shows a schematic sketch of a mechanical gripper system with its components. The individual subsystems are listed below and described in more detail below.

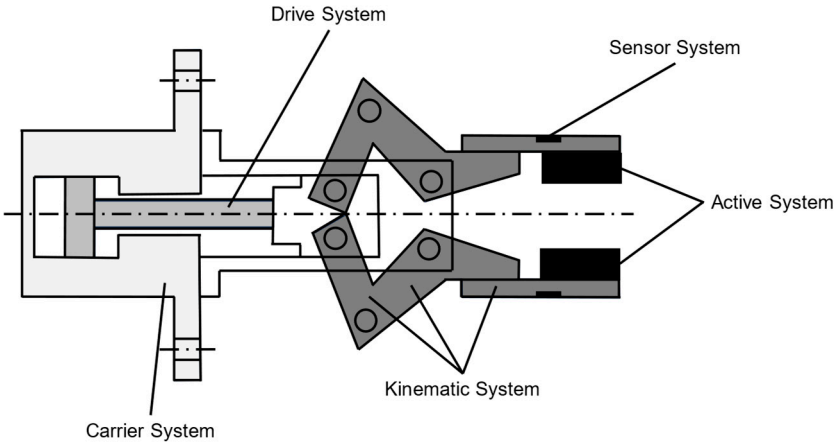

Figure 2. Schematic representation of an exemplary gripper system and its components (own presentation) [24].

Carrier System

The carrier system creates a secure connection between the gripper system and its surrounding system, usually in the form of a flange. Other tasks include the supply of drive energy and a connection between the sensors and the control system [23,24].

Drive System

The selection of a suitable drive system is a key aspect in the development of automation solutions and has a significant influence on their functionality. The drive system converts the supplied energy into rotational or translational kinetic energy, which then generates the gripper movement [23,24].

Kinematic System

The kinematic system comprises all the components required to convert the movement of the drive system into a movement of the holding system. An important feature is the transmission ratio between the drive system and the active system. Within the kinematic system, there are various options for adjusting the force/displacement ratio of the gripper [23,24].

Active System

The part of the gripper system that has direct contact with the object is the holding or active system. A mechanical gripper introduces the clamping force via the active surfaces of the gripper links. As with the overall system, the tasks are to establish and release contact with the object [23,24].

Sensor System

The task of this subsystem is information processing. By default, the gripper is controlled via a higher-level handling device. Sensors can be used to check the position of the object or the status of the holding system. This information can be read out by the control system and the overall system can be controlled [23,24].

2.3. State of the Art for Grippers with Shape Memory Alloys

There are not many grippers for automation technology that are powered by SMA and are commercially available. The only systems available on the market are micro grippers. Glashütte offers different versions of microgrippers based on the SME. Components in the 10 µm range are gripped with a force of up to 500 N [26].

In the field of research, different types of grippers based on SMA have already been considered. Scholtes et al. 2021 developed a gripper with a slightly larger stroke (6.4 mm) compared to the aforementioned microgrippers. It is a solid-state joint gripper driven by SMA. The use of wire bundles increases the available force, but at the same time achieves a low switching frequency [27]. Lu et al. 2019 developed a gripper with a large stroke by connecting several SMA wires in series and, thus, enabling a large gripping opening by summing up the strokes [28]. However, due to the complexity of the design, this approach runs counter to the actual advantages of SMA, which are the small installation space required and their light weight. With flexible gripper fingers and the requirement for a small installation space with a light weight, Zhou and Ma 2022 developed a flexible SMA-wire-based gripper. Using a transmission ratio, they enabled a gripper opening of 14 mm in contrast to the 2 mm stroke generated by the wire [29]. However, grippers driven by SMA springs have also been developed [30,31]. The advantage of springs is that they generate a larger stroke, but they generate less force and are more complex to manufacture [32].

Other gripping principles have also been considered. A soft gripper driven by SMA was developed by Lee et al. (2019). Using a combination of moving and rigid elements, they generate a transmission ratio to transfer the low stroke of the wire into a high bending angle [33]. Li et al. 2024 developed another soft gripper capable of achieving an opening width of over 15 mm per finger and generating a force of up to 0.12 N at the fingertips. To facilitate these dimensions, a long wire is used, which is redirected multiple times [34].

A pneumatic gripper was also developed using SMA. By activating the SME, Motzki et al. (2020) generate a vacuum on suction cups, which pneumatically holds the component [35]. Table 1 compares various SMA grippers in terms of their dimensions. Additionally, examples of one electric and one pneumatic gripper are compared. It becomes evident

that SMA grippers are either small and lightweight, but with a limited opening width, or they have a large opening width but are consequently large and heavy.

Table 1. Comparison of different grippers.

Label	Weight [g]	Size [mm]	Opening Width [mm]	Gripping Force [N]
		SMA Actuator		
WPT/6 [26]	3	41 × 9 × 6	1	0.2–0.8
BPT/3 [26]	18	56 × 27 × 15	2	100
KHG/3 [26]	20	59 × 33 × 14	3	10–500
Scholtes et al. [27]	150	100 × 100 × 10 *	6.4	n.s.
Lu et al. [28]	2564	206 × 90 × 182	60–100	4–7.5
Zhou and Ma [29]	n.s.	120 × 30 × 10 *	14	1.2
		Electric Actuator		
2FG7 [36]	1100	144 × 90 × 71	39/ 73	20–140
		Pneumatic Actuator		
PGL-plus-P 20-IOL [37]	2700	191 × 83 × 59	40	880
		New Actuator (developed in this work)		
	107	46 × 60 × 23	40	1.25

* Dimensions were estimated based on the illustrations and information provided.

A two-finger gripper driven by SMA wires with an opening width of up to 40 mm is not yet available for purchase, nor has it been scientifically investigated.

Beyond automation technology, grippers are utilized in various other fields. Consequently, robotic or prosthetic arms driven by SMA, which function as grippers, were also be considered. These devices are primarily developed for application in the rehabilitation of patients following strokes or limb amputations [38]. In many cases, SMA springs are used instead of wires to generate larger actuation displacements [39–41]. For rehabilitation purposes, Wang et al. (2021) developed an artificial hand actuated by SMA wires, which is utilized in the rehabilitation field. Due to the apparatus requirements arising from the operating conditions, a compact design is not necessary, resulting in a structure with a length exceeding 300 mm [42]. Hadi et al. (2017) developed a similar setup, attempting to reduce the actuation unit's size through pulleys. Nevertheless, the actuator measures 240 mm in length, without incorporating any gripping fingers [43]. Actuators inspired by the human hand have also been developed for grasping objects. These actuators can achieve openings of up to 8 cm through finger rotation [44,45]. By implementing SMA wires directly into the gripping fingers, Simone et al. were able to reduce the size of the unit to 200 mm and achieve a weight of 300 g [46].

As these grippers were originally conceived for a different purpose accompanied by non-comparable requirements, their direct applicability to automation technology is limited. Furthermore, they are often characterized by high complexity and weight. Nonetheless, these designs serve as valuable contributors to the generation of ideas in the ongoing trajectory of development, which serves as the basis for the development elaborated in this work.

3. Materials and Methods

The development of the gripper presented was carried out systematically. Functional structures were derived based on a list of requirements and, ultimately, different variants were developed from a morphological box. The list of requirements was based on the requirements arising from using SMA and the requirements from the field of automation technology, such as the available electrical connection or the ambient operating temperature, while weight and size should be as low as possible. Furthermore, requirements derived from the comparison of currently available gripper systems on the market, which are not yet driven by SMA grippers, were also used. These requirements, which, for example,

include a large opening width of up to 40 mm as well as a low weight and compact design, constitute the primary focus of the innovation aspects.

The different variants were then evaluated on weighted criteria from the list of requirements. During the evaluation process, the methodology of point rating, as described in the design theory by Pahl and Beitz, was employed. This involved team deliberations to assess individual solution variants, where the attributes of each variant were delineated and subsequently evaluated through point allocation for finding the best possible solution [5].

Based on this analysis, the overall utility value of the solution using a gear transmission in combination with lever arms is significantly higher than that of the other solutions developed. In addition, it meets all the necessary minimum requirements, which is why this variant was chosen for further development and is presented below.

3.1. Mechanism Design

The mechanical design of the new gripper is presented and explained below. Figure 3 shows the kinematic system of the gripper.

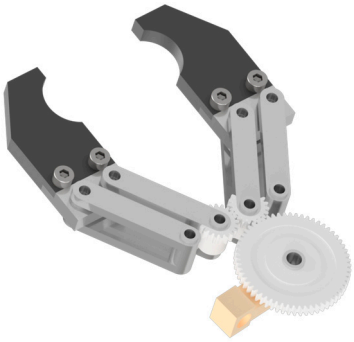

Figure 3. Kinematic system of the new gripper design.

The design of the mechanical components starts with the consideration of the given boundary conditions. These include the requirements from the specifications, the operating principle from the selected solution variant, and the dimensions of the existing and selected components. A transmission with a gear stage in combination with a lever arm must be designed.

The maximum wire length L (150 mm) and the maximum elongation ε (4%) of the wire can be used to determine the stroke generated by the wire according to Formula (1).

$$s_{stroke} = L_{wire} \cdot \varepsilon_{max} = 150\ \text{mm} \cdot 0.04 = 6\ \text{mm} \quad (1)$$

Based on the calculated stroke and the required opening width of the gripper of 40 mm, the required total transmission ratio of the system is then determined. The opening width of the gripper fingers is achieved by two fingers, so this is divided into 20 mm per finger. Therefore, the transmission ratio, i, of the gear drive is first determined using Formula (2).

$$i = \frac{s_{output}}{s_{input}} = \frac{20\ \text{mm}}{6\ \text{mm}} = 3.\overline{33} \quad (2)$$

A module of 0.5 was chosen for the selection of the gears. Due to the relationship between the module and the diameter of a gearwheel, these are correspondingly smaller. Gears with 60 and 20 teeth were selected for this purpose. The driving force acts on the gearwheel with 60 teeth, and the gripper fingers are connected to the pinions.

The radii and dimensions of the gears can be calculated using the module; for the sake of simplicity, they can be taken from the data sheets and are summarized in Table 2.

Table 2. Geometric properties of the gears.

	Gear	Pinion
Number of teeth	60	20
Bore diameter	6 mm	4 mm
Pitch diameter	30 mm	10 mm

The center distance of the two pinions, one for each finger, is 10 mm. Once the gear wheel alignment has been calculated, the required angle of rotation of the gear wheel is determined using the gripper finger length to achieve the required positioning movement of 20 mm. The finger length is the sum of the holding arm length and the actual finger length. The length of the fingers is 70 mm, of which 40 mm is accounted for by the gripper fingers and 30 mm by the arms. The length of the holding arms is used for the calculation. Figure 4 illustrates the structure of the holding arms in a polar coordinate system.

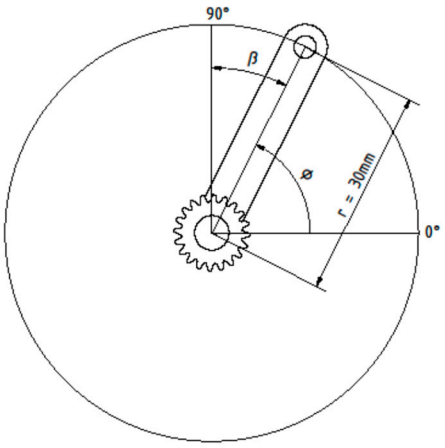

Figure 4. Sketch for calculation of the holding arms.

Formulas (3) and (4) are used to convert cartesian coordinates into the polar coordinate system, where r denotes the radius and Φ the angle of rotation:

$$x = r \cdot \cos \Phi \tag{3}$$

$$y = r \cdot \sin \Phi \tag{4}$$

To calculate the angle of rotation required to achieve an opening width of 20 mm, the formulae must be rearranged (s. Formulas (5) and (6)).

$$\Phi = \arccos \frac{x}{r} \tag{5}$$

$$\Phi = 48.19^\circ \tag{6}$$

The required angle, β, results from the sum of the angles in a triangle. To generate the required stroke of the fingers, the gear must rotate by at least $\beta = 41.81^\circ$. From this point, a safety factor is built in by assuming an angle of $\beta^* = 45^\circ$. Using the transmission ratio, i, the angle of rotation, δ, of the large gear can be calculated to determine β^* according to Formula (7).

$$\delta = \frac{\beta*}{i} = \frac{45^\circ}{3} = 15^\circ \tag{7}$$

The required lever arm length can be determined by the angle of the wheel and the generated stroke of the SMA actuator. Figure 5 shows the corresponding values. The required length of the lever arm, r_{arm}, indicates the point at which the force acts on the SMA actuator on the lever arm.

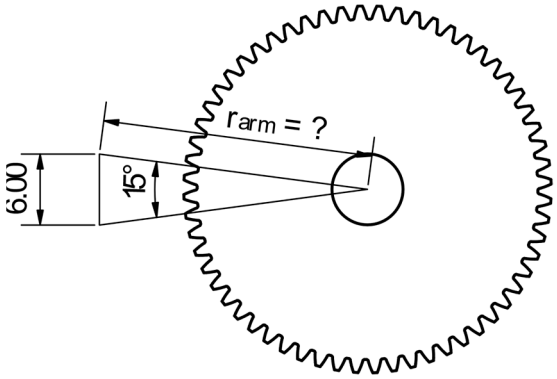

Figure 5. Sketch for calculation of the lever arms.

A triangle is formed from the generated stroke s = 6 mm, the radius of the point of application, and the angle δ = 15° between the maximum positions of the lever arm. By using the sine theorem, a lever arm length of r_{arm} = 22.98 mm can be determined. To take an additional safety factor into account, a lever arm length of r_{arm} = 20 mm is assumed, as the lever law results in a higher angle of rotation with a shorter lever arm.

The built-in safety factors in the form of oversizing serve to compensate for losses, for example, due to friction or fatigue effects of the SMA wire. To determine the safety factor, the calculation is carried out again with a lever arm length of r_{arm} = 20 mm. This results in a movement of 23.56 mm for each of the two gripper fingers. A comparison with the nominal value results in a safety factor of 1.17.

3.2. Design of the Gripper

The gripper is designed in CAD using the previously defined dimensions and units before it is manufactured and tested as a prototype. The design and functionalities can also be evaluated in CAD. Figure 6 shows the final design of the gripper.

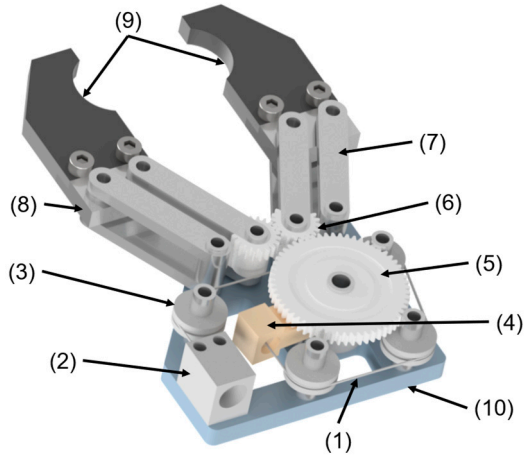

(1)	SMA wire
(2)	Holding block
(3)	Pulley
(4)	Lever arm
(5)	Gear wheel
(6)	Pinion
(7)	Connection arms
(8)	Finger holder
(9)	Finger
(10)	Base plate

Figure 6. CAD illustration of the gripper with list of parts.

The SMA wire (1) is connected to the actuator on both sides, whereby one side is fixed and the other is loose. On the firmly clamped side, the wire is tightened by two holding blocks (2) and a crimp. The wire can also be re-tensioned within these holding blocks via an adjusting screw if the wire fatigues in the form of elongation over the lifetime. To reduce the installation space, the wire is deflected over several pulleys (3). On the loose side, the wire is attached to the lever arm (4) via a crimp. The lever arm transmits and transfers the force of the wire as a torque to the gear wheel (5). A torsion spring is mounted under the gear wheel, which is required to reset the SMA effect and automatically close the gripper. From the gear wheel, a transmission takes place to the first pinion (6), which transmits a 1:1 ratio to the second pinion

for the second finger. The connecting arms (7) are embedded in the pinions and connected to the finger holders (8) on the other side. Fingers (9) with different shapes can be attached to the finger holders to generate a form fit with the object to be gripped. All elements are mounted on a base plate (10) and are countered by a cover plate.

3.3. Evaluation of the Opening Width in CAD

The requirement for the gripper to achieve an opening width of 40 mm was considered in the design and construction. In addition, an evaluation was carried out on the CAD model as part of the design. Figure 7 compares the gripper in the open and closed state. The activation of the wire is represented by the rotation of the lever arm by 15°.

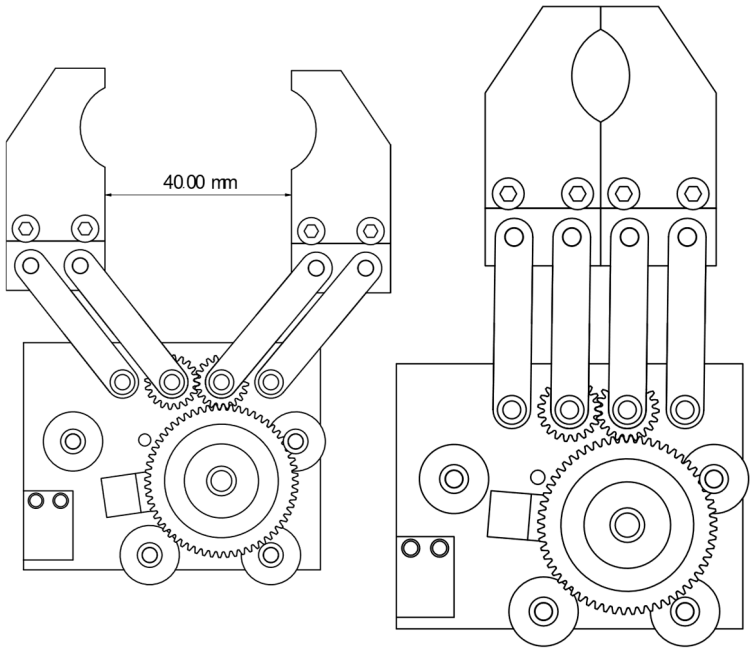

Figure 7. Evaluation of the opening width in CAD (**a**) fully opened (**b**) closed.

3.4. Force Curve in the Gripper

The force curve in the gripper is examined closer to illustrate the functionality of the gripper; the forces generated and working in the system are plotted and described. The gripper system is considered from the applied force of the wire to the opening of its fingers. Figure 8 shows the forces applied to the gear wheel.

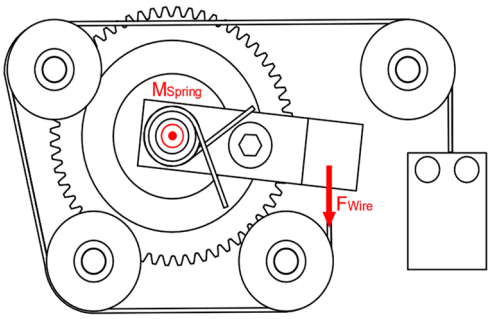

Figure 8. Force curve of wire and counter spring.

To open the gripper, the wire is activated and generates the force, F_{Wire}. This force generates a torque on the gear wheel via the lever arm, which works against the torque applied by the torsion spring. The sum of the torques produces a resulting torque, which

is transmitted to the fingers via the kinematic system. The forces in the upper part of the system are shown in Figure 9.

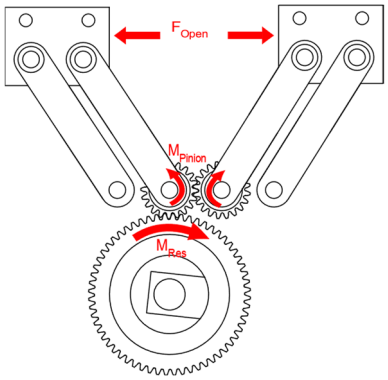

Figure 9. Force curve via gearwheel and pinion to the gripper fingers.

The resulting torque (M_{Res}) of the gear wheel is transmitted to the pinions. The pinions transmit the torque (M_{pinion}) to the connecting arms, causing the grippers to open with the force F_{Open}. When the gripper is to be closed, the actuator is deactivated, and the force, F_{Wire}, slowly approaches 0 N due to the cooling of the wire. This changes the direction of the force of the resulting torque and the gripper closes again. Both the selection of the torsion spring and the selection of the diameter of the wire are relevant for determining the forces and torques, as these two factors influence the force. As the wire must work against the torsion spring during each activation, the force applied by the wire must be greater than the counterforce of the torsion spring. In the following, only the force curve during closing by the torsion spring is considered, as this is only relevant in the application, in contrast to the force generated by the gripper during opening.

The torsion spring selection was designed to ensure that the spring force is sufficiently large to reset the SMA wire while remaining smaller than the SMA force during activation. During this design of the forces, the manufacturer's specifications were used as a guide [47]. This ensures that adequate wire force is available for the movement of the gripping fingers. Depending on the wire diameter and the spring's dimension, the resulting gripping force was calculated for different springs. The calculation for the torsion spring used will be explained in further detail.

The resulting force on the gripper fingers is calculated using the Formulae (8)–(11). The torsion spring is installed so that it is preloaded by 42.4° at an opening width of the gripper fingers of 40 mm. At this elongation, the spring generates a torque of 350 Nmm on the wheel. The calculated angle of rotation of the wheel of δ = 15° results in an elongation of the gearwheel with closed gripper fingers of 27.4°. At this elongation, the torsion spring generates a torque of M_{Spring} = 226.32 Nmm.

$$M_{Gear_{Closed}} = \frac{1}{i} \cdot M_{Spring} = \frac{1}{3} \cdot 226.32 \text{ Nmm} = 75.44 \text{ Nmm} \quad (8)$$

This results in a torque on the pinion of $M_{Gear\ Closed}$ = 75.44 Nmm, which is distributed over the two pinions. Using the lever law, the torque is converted into the acting force of the gripper fingers. The torque is transferred to the fingers with a lever arm of r = 20 mm. The calculation of the force on the fingers in the closed state is shown in Formula (9).

$$F_{Closed} = \frac{M_{Gear_{Closed}}}{r} \cdot \frac{1}{2} = 1.25 \text{ N} \quad (9)$$

Formulas (10) and (11) can be used to determine which weights, m, can be held under force, and the coefficient of friction, μ, depends on the material pairing. If the shape of the

gripper fingers is adapted, objects can also be held by positive locking, so the closing force would not be relevant.

$$m \cdot g < F_{Friction} \tag{10}$$

$$F_{Friction} = \cdot N = \cdot F_{Closed} \tag{11}$$

3.5. Space and Weight Reduction Within the Design Process

To reduce the installation space and weight, the wire was deflected several times in the design. To compare the reduction, a version of the gripper was also constructed, which does not have a deflection of the wire. Both versions are shown with dimensions in Figure 10. As the fingers are identical in both versions, they are not included in the comparison and only the size of the SMA actuator is considered.

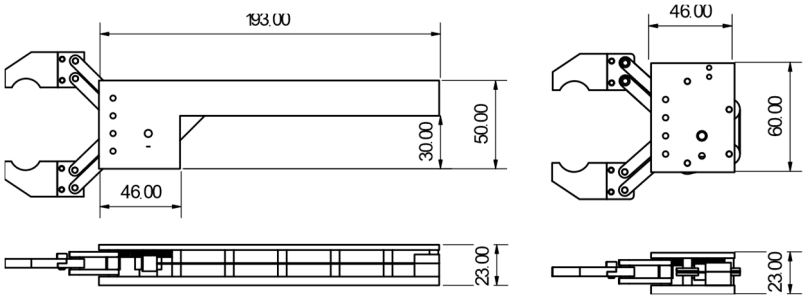

Figure 10. Size comparison of the two gripper variants (**a**) with installation space not reduced and (**b**) with installation space reduced.

Table 3 compares the respective dimensions together with the calculated volume.

Table 3. Installation space of the two gripper variants (without the fingers).

	Installation Space Not Reduced	**Reduced Installation Space**
Length	193 mm	46 mm
Wide	50 mm	60 mm
Height	23 mm	23 mm
Volume	120.50 cm^3	63.48 cm^3

The table shows that the length of the gripper is reduced by 76.17 %, this significant difference is due to the deflection of the wire in the kinematic system. The width of the gripper increases by 20 % due to the space required for positioning the pulleys. However, the increased width is not problematic as it is still less than the width of the gripper fingers at maximum opening and, therefore, has no negative impact. The systems do not differ in height. The respective installation space volume can be determined from the dimensions of the gripper, whereby the installation space between the plates is considered. For the version without reduced installation space, it must be noted that the volume cannot be calculated directly from the maximum length and width due to the cut-outs. This results in a volume of 120.5 cm^3 for the gripper without and 63.48 cm^3 for the variant with reduced installation space. This means that a reduction in installation space of 47.3 % could be generated by deflecting the wire. However, the deflection adds further components, which increases the complexity and weight. In addition, the influence of a deflection on the lifetime of the wire and, therefore, the gripper is unknown.

To determine the total weight, the masses of the individual components are added together; these are determined with the help of data sheets, supplier information, and CAD software (Autodesk Inventor Professional 2023). Table 4 shows the parts list of the two variants together with the weights of the individual components.

Table 4. Parts list with exemplary components that have the main influence on the weight.

	Reduced Installation Space			Installation Space Not Reduced		
Item Number:	**Quantity:**	**Weight: [g]**	**Sum: [g]**	**Quantity:**	**Weight: [g]**	**Sum: [g]**
M3x25	8	1.4	11.2	9	1.4	12.6
M4-Nut	8	0.7	5.6	9	0.7	6.3
D5 Distance Sleeves L = 7	4	0.09	0.36	2	0.09	0.18
D6 Distance Sleeves L = 15	1	0.6	0.6	9	0.6	5.4
D5 Distance Sleeves L = 5.5	8	0.07	0.56	-		
Base Plate	1	23.427	23.427	1	69.15	69.15
Ball Bearing	4	1.6	6.4	-		
Cover Plate	1	9.47	9.47	1	17.692	17.692
...	...	...	...	...	...	...
Total weight:			**106.877**			**160.402**

A weight reduction of 33% could, therefore, be achieved. The differences in weight are mainly due to the dimensions of the base/cover plate. In both variants of the gripper, the weight can be further reduced by suitable design measures; for example, by using other materials or by inserting additional cut-outs in the plates, as shown in the base plate in Figure 11. By adapting the base plate and cover plate, a further 10.38% of the weight could be reduced.

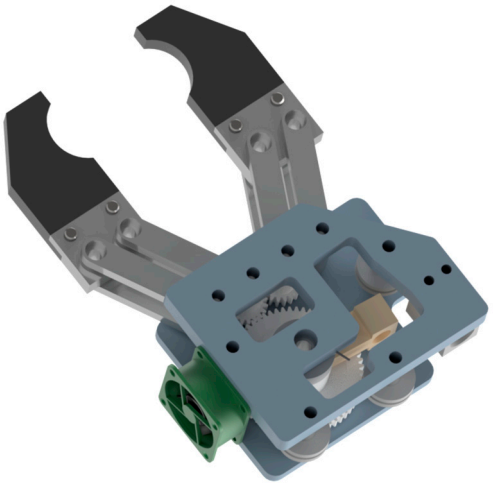

Figure 11. Optimized version of the gripper in CAD with weight reduction, deflection, and fan.

The potential effect of wire redirection on performance is not considered here. Redirecting the wire to reduce installation space is a common design practice, but its effects are not well understood. Contact with the material of the pulley component may result in altered heat flow, or the material pairing with NiTi may result in degradation of the wire or pulley due to wire cutting into the surface.

4. Development and Evaluation of a Prototype

A prototype was built to evaluate the developed gripper, which will be evaluated in long-term tests (Figure 12). The cover plate for the prototype was made of plexiglass to make it easier to visualize how the SMA actuator works. The connecting arms were also cut out of plexiglass using a laser cutter, as this made production easier and faster. The ball bearings and gears were purchased, whereby the gears were re-machined to enable the gripper arms to be accommodated. Sleeves made of Polyoxymethylene (POM) were placed

on the ball bearings for insulation during electrical activation, ensuring that the current for activating the wire is not dissipated.

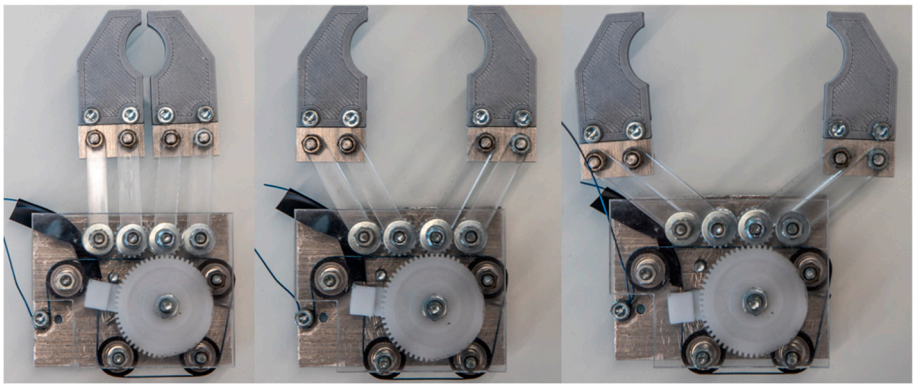

(**a**) (**b**) (**c**)

Figure 12. Pictures of the prototype with different opening widths, which were set mechanically and not by an SMA wire. (**a**) Fully closed; (**b**) 30 mm opened; (**c**) maximum opening width of 50 mm. A video of the actuator in operation can be found in the Supplementary Material.

A Flexinol actuator wire from DYNALLOY, Inc., Irvine, CA, USA [47] with a diameter of 0.5 mm was used as the actuator for the prototype. The wire was held in the lever arm by a crimp. Contrary to the actual design, the other side of the wire was clamped to a screw for the prototype, making it easier to tighten the wire in the test phase.

To evaluate the development and the prototype, a test rig was setup and several test series and long-term tests were carried out. Therefore, the gripper is mounted on a plate and the wire is connected to a power supply unit. The power supply unit can be switched on and off via a relay circuit to activate the wire when energized and cooled down when the relay is off. Another small and lightweight plate is attached to one side of a gripper finger, onto which a laser displacement sensor is directed. The stroke of one gripper finger can be recorded via this sensor. Due to the 1:1 ratio of the pinions to each other, both gripper fingers move in the same way, so that the path recorded by the laser path sensor can be doubled to determine the opening width of the gripper. In addition, a fan is installed on the test rig, which enables a series of tests with accelerated cycle times. To activate the wire, 3.6 V was applied to the wire for a duration of 4 s. The chosen parameters were determined for the material used in preliminary experiments and other studies. The design was carried out in such a way that a complete activation of the wire occurs during each cycle. The activation time of 4 seconds was chosen to ensure the movement and behavior of the gripper is clearly observable and understandable.

4.1. Testing the Opening Width of the Prototype

In addition to evaluating the opening width using the CAD model, an evaluation is also carried out on the prototype. The opening width of the gripper in the first 30 cycles is shown in Figure 13. The gripper starts in the closed state and, therefore, with an opening width of 0 mm. During the first activation, a movement of each gripper finger of 15.3 mm and, thus, a total width of 30.6 mm is generated. Subsequently, the gripper does not close completely and remains open by 1.5 mm. Looking at the opening width in the closed and open state of the gripper, it can be seen that the gripper closes less and less over the number of cycles, although the opening width remains almost constant. At the 30th cycle, the gripper remains open by 3.6 mm with a maximum opening width of 29.6 mm. As a new wire is used for the test series, it can be assumed that the fact that the gripper no longer closes completely is due to the run-in effect of the wire. It is caused by an accumulation of dislocations, which induce residual deformation and the formation of stabilized martensite. These changes in the microstructure lead to altered behavior, resulting in reduced functional

properties [48]. The backlash of the gearwheels also affects the gripper's ability to close completely, as the movement and force of the gearwheel is not fully transmitted to the pinions until the end.

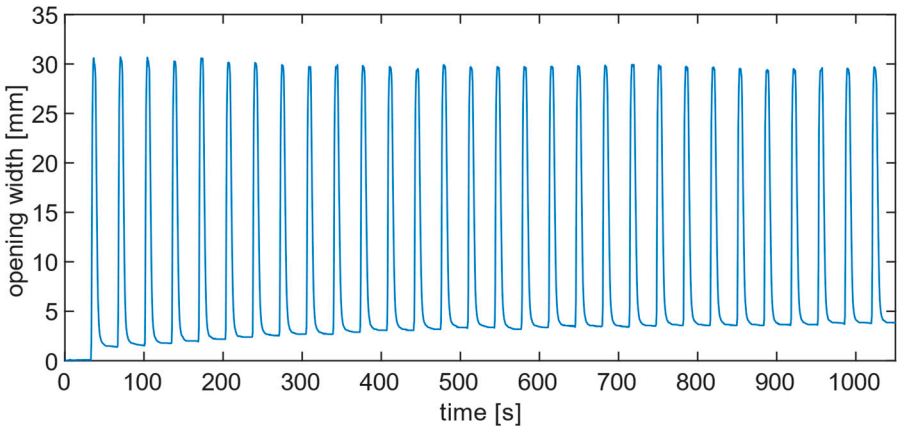

Figure 13. Opening width of the gripper over the first 30 cycles.

4.2. Examination of the Cycle Time and Possible Frequency

A relevant requirement for the gripper in the application is the operating time that the gripper needs to open and close. The operating time depends on the activation speed of the wire. The activation of the wire can be accelerated by increasing the electrical voltage. This has already been demonstrated by Czechowicz et al. [49], which is why the activation duration is not considered below. The deactivation time of the actuator is based on cooling by free convection, during which the heat of the wire is released into the environment. To shorten the deactivation time, it is possible to direct a fan at the gripper system, which generates an airflow across the gripper and accelerates the cooling of the wire by forced convection [50]. To investigate the influence of the fan, two series of measurements with and without the fan are shown below. The first five activations of each series of measurements are shown in Figure 14, with each activation lasting 4 s and a cooling time of 30 s between each activation.

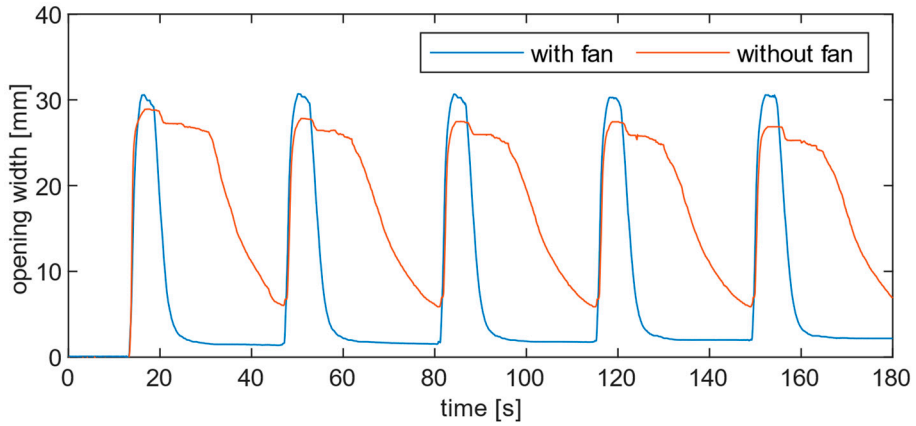

Figure 14. Opening width of the gripper at different cooling speeds with and without a fan.

In both cases, a rapid opening of the gripper resulting from a rapid activation of the wire can be seen. The clear difference can be found in the speed during cooling. While the actuator without a fan is still not completely cooled down after 30 s—recognizable by the fact that no limit value is reached—the actuator is already back in its initial state after about 5 s when the fan is switched on. Since the fan was running continuously, even during wire activation, a reduced maximum opening width would be expected as the thermal energy

required to activate the effect is dissipated by the increased forced convection. The reduced maximum opening width in the test series without a fan compared to the one with a fan might have been attributed to a different tensioning of the wire since the test series were carried out with a new wire each.

As the wire is reset by the opposing spring during the cooling process, which is supported by the fan, in approximately 5 s, the frequency could be almost doubled. For an optimized airflow and improved cooling of the wire in the housing, a fan was added to the housing of the actuator in Figure 11 to illustrate a possible solution variant. This positioning of the fan does not interfere with the mechanical gripping process. The dimensions of the fan have been adapted to the installation space of the gripper and measure 20 mm × 20 mm so that it can be easily attached to the side of the gripper. The cooling time can be further optimized and reduced by directing the airflow in a targeted manner.

4.3. Long-Term Investigations

Several long-term tests were carried out. In these test series, up to 19,472 activation cycles were achieved before the actuator failed. In the case of failure of the wire itself, this was due to fatigue of the SMA wire, which failed at the temporary clamping between the screw and nut. In other long-term tests, the crimp or screw came loose, but the mechanics of the actuator remained unaffected in all cases.

Figure 15 shows the course of the maximum and minimum opening width of the gripper over the long-term test of 19,472 cycles with the fan. The minimum opening width shows that the gripper is only completely closed in the first cycle (before the first electrical activation). From the second cycle onwards, a residual opening width of approx. 12 mm remains, even when the wire is completely cooled down by the use of a fan. This is based on the running-in effect of the wire, but more strongly due to the backlash in the gears, which leads to a significant loss of the maximum opening width, particularly during the first activation cycle (as seen in Figure 15). As a result, the gripper no longer closes completely because the gear is pushed back by the spring, but a complete transfer to the pinion does not occur. A similar progression can be seen with the maximum opening width. There, the maximum opening width increases by approx. 5 mm within the first 200 cycles. This can be attributed to the running-in effect of the SMA wire [51], which adapts its functional properties to the respective load within the first few cycles. Gear backlash and prototype manufacturing also play a role in the maximum opening width, resulting in a reduced opening width. When the prototype is operated manually, a backlash of the gears can be determined resulting in an opening width of the gripper fingers of approximately 12 mm. The gripper can be opened manually to this extent without the pinion movement being transmitted to the gear. This opening width of 12 mm must be taken into account as an inaccuracy in the theoretical opening width from Chapter 3 compared to the opening width of the prototype. Without this backlash, the prototype would close and further open up to 12 mm.

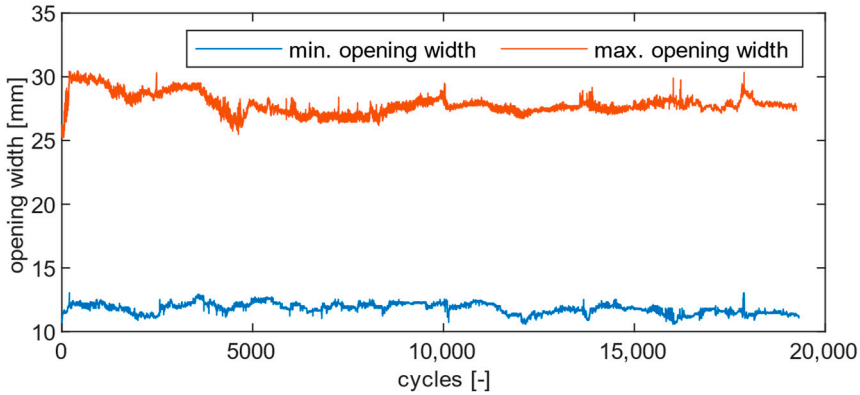

Figure 15. Minimum and maximum opening width of the gripper in a long-term test over the lifetime of the wire.

The resulting opening width of the gripper can be determined by the difference between the maximum and minimum opening width. Figure 16 shows the curve together with a regression line. The regression line can be used to determine that the resulting opening width is 16.14 mm on average and is not subject to any major change over the activation cycles. The different characteristics of the run-in effect of the maximum and minimum opening width over the cycles clearly show the delayed run-in effect in the resulting opening width.

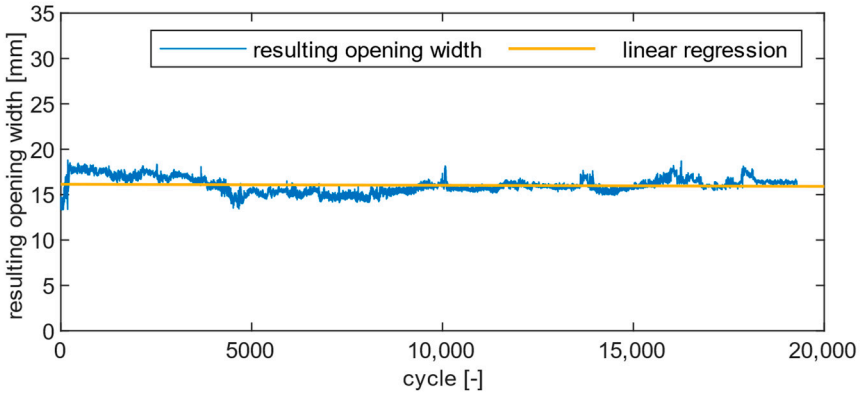

Figure 16. Resulting opening width with compensation line over the lifetime of the wire.

However, regarding the gripper's application, gripping of objects, it should be noted that the maximum opening width is more relevant than the resulting opening width. The maximum opening width defines the maximum size of objects that can be gripped, whereas not completely closing the gripper has no influence on gripping as long as the object to be gripped is larger than the minimum opening width caused by the influence of the run-in effect. Nevertheless, the run-in effect can be averted by the deployment of pre-trained wires or by readjusting the wire during usage and backlash can be improved by optimizing the production of each component.

5. Discussion/Summary

The use of SMAs as a drive system in gripper mechanisms is based on their high energy density, allowing for significant improvements in existing technical applications, particularly in terms of weight reduction and minimized installation space. This results in the requirement to develop a gripper system driven by SMA wires.

Research into the state-of-the-art shows that, with a few exceptions, there is yet no commercial market for SMA actuators. In the field of research, there are many application areas for SMA. There are several approaches in the field of gripper systems, with miniature grippers and soft grippers being developed. During the research, no gripper systems were found operating with SMA and corresponding to the opening width (up to 40 mm), low weight (107 g), and size as achieved with the new gripper presented in this work.

To ensure an optimal procedure, various methods from VDI guidelines and product development were combined and brought together in an adapted model. With the help of this model, a structured and efficient development process was enabled to find the best solution possible, while the methodical approach makes it possible to generate a solution as objective as possible.

In CAD, a version was developed in which the wire actuator is installed at its full length; in a second variant, the wire was deflected with a pulley system. The aim is to deflect the wire so that the installation space of the overall system is reduced. The weight and volume of the variants were determined using the CAD program. The results show that a lightweight gripper has been developed that can even be further optimized. Regarding the installation space, it was demonstrated that the redirection of the wire actuator achieves an enormous volume saving.

The design of the gripper was described in detail and the knowledge gained during the design process was presented. The prototype was built, and functional tests were carried out. The tests have shown that the prototype achieves an opening width of 30.6 mm. and no longer closes completely after a certain number of cycles. The activation and deactivation times with and without ventilation were also investigated. In the absence of ventilation, the gripper requires 16.1 seconds to close. In contrast, when ventilation is present, the cooling process is markedly enhanced, and the deactivation time is reduced to 4.6 seconds. In the future, the activation speed can be accelerated by faster electrical activation [49]. The cooling speed can also be accelerated by up to 25 times by using an adapted cooling method [47].

The evaluation of the developed and realized prototype reveals potential areas for improvement and opportunities for further investigation. The functional tests on the prototype show that the required opening width was not achieved, which can be caused by various factors. Firstly, the components are not optimally manufactured. It has been shown that the friction on some components is greater due to manufacturing tolerances. As a result, the force of the spring is required to overcome these frictional forces. Another factor is the materials used. The gear wheels are made of plastic and exhibit a high degree of backlash. The lever arm is also made of plastic, whereby the resulting forces—especially of the spring—lead to deformations that can cause further inaccuracy, which is also visible with the prototype. For improved functionality, the gears should be manufactured and implemented with tighter tolerances and the lever arm should be made of a stronger material.

6. Conclusions and Outlook

The two-finger gripper presented in this work is the first of its kind to offer a large opening width of up to 40 mm, a notable advancement over existing literature and products on the market. Despite this expansive opening, the gripper maintains a compact and lightweight design, weighing just over 100 grams (see Table 1). Although the prototype exhibits a reduced opening width of 30 mm, the underlying reasons for this and the means of attaining the desired opening width of 40 mm were subjected to a comprehensive examination. Nevertheless, an opening width of 30 mm with the low weight represents a novel development in comparison to existing SMA actuator principles. This paves the way for new applications in the field of automation technology where larger opening widths but low weight are required. The opening width of the actuator can also be scaled by adjusting the transmission ratio—in particular the size and number of teeth of the gears.

The functionality and operation of the actuator have been proven in various test series. The durability has also already been demonstrated on a prototype. During long-term testing of the prototype, it became evident that measures needed to be taken to anticipate the "run-in" effect for stable operation with a repeatable opening width. This could be achieved through tailored training of the actuator during the manufacturing process or by readjusting the wire during operation. However, the lifetime must be further increased for economical use. In particular, the weak point of the clamping on the prototype must be implemented as planned in the actual design to achieve the required lifetime, as the wire failed there on the prototype. In addition, further influences on the lifetime of the wire in the actuator must be investigated. For example, it is not yet known how the deflection of the wire affects the lifetime and functional properties of the wire. Due to a contact surface to the pulley and the induction of mechanical stress in the wire by bending, the wire is subjected to a load with an influence on fatigue behavior that has not yet been fully investigated. However, initial preliminary work has shown that deflections have a negative influence on lifetime [52]. By optimizing the design based on the empirical values of the prototype with an optimized selection of materials and manufacturing tolerances, it can be assumed that the opening width of 40 mm can be achieved. Through improved material pairing, friction losses are minimized, allowing for greater translation of force into displacement. Additionally, the plastic gears used exhibit significant optimization

potential, as they currently have considerable clearance. This would further reduce losses and maximize the opening width.

Furthermore, the objective is to determine the gripper's opening width based on the wire's electrical resistance, eliminating the need for additional sensors. Changes in the material's phase transformation result in alterations in its specific resistance, which can be correlated with the wire's displacement and, thus, the gripper's opening width.

Common drawbacks of NiTi SMA, such as low actuation frequency due to thermal activation and cooling of the material and degradation of functional properties over time, need to be further addressed in scientific research to promote their economic application.

Supplementary Materials: The following supporting information can be downloaded at: https://www.mdpi.com/article/10.3390/act13100425/s1, Video S1: Actuator prototype in use.

Author Contributions: Conceptualization, T.S.; methodology, L.B. and T.S.; software, T.S.; validation, L.B. and T.S.; formal analysis, L.B. and T.S.; investigation, L.B. and T.S.; resources, B.K.; data curation, L.B. and T.S.; writing—original draft preparation, L.B. and T.S.; writing—review and editing, B.K.; visualization, L.B. and T.S.; supervision, B.K.; funding acquisition, B.K. All authors have read and agreed to the published version of the manuscript.

Funding: This research work was funded by the Deutsche Forschungsgemeinschaft (DFG, German Research Foundation) within the research project "Gekoppelte funktionelle und strukturelle Ermüdung (GFSE) von Formgedächtnisaktoren" (project number 498172553). The authors thank the DFG for promoting and financing the research.

Data Availability Statement: Data are contained within the article.

Conflicts of Interest: The authors declare no conflicts of interest.

References

1. Boshoff, M.; Miro, M.; Sudhoff, M.; Kuhlenkötter, B. Use of Autonomous UAVs for Material Supply in Terminal Strip Assembly. In *Annals of Scientific Society for Assembly, Handling and Industrial Robotics 2022*; Schüppstuhl, T., Tracht, K., Fleischer, J., Eds.; Springer International Publishing: Cham, Switzerland, 2023; pp. 355–365. ISBN 978-3-031-10070-3.
2. Verein Deutscher Ingenieure. *Produktentwicklung mit Formgedächtnislegierungen (FGL)*; Beuth Verlag GmbH: Berlin, Germany, 2017; 77.100, 77.120.99 (2248-1). Available online: https://www.vdi.de/richtlinien/details/vdi-2248-blatt-1-produktentwicklung-mit-formgedaechtnislegierungen-fgl-grundlagen-und-anwendungsbeispiele (accessed on 16 October 2024).
3. Verein Deutscher Ingenieure. *Produktentwicklung mit Formgedächtnislegierungen (FGL)*; Beuth Verlag GmbH: Berlin, Germany, 2017; 77.100, 77.120.99 (2248-2). Available online: https://www.vdi.de/en/home/vdi-standards/details/vdi-2248-blatt-2-product-development-using-shape-memory-alloys-sma-material-selection-and-nomenclature (accessed on 16 October 2024).
4. Verein Deutscher Ingenieure. *Produktentwicklung mit Formgedächtnislegierungen (FGL)*; Beuth Verlag GmbH: Berlin, Germany, 2017; 77.100, 77.120.99 (2248-3). Available online: https://www.vdi.de/en/home/vdi-standards/details/vdi-2248-blatt-3-product-development-using-shape-memory-alloys-sma-test-and-measurement-methods (accessed on 16 October 2024).
5. Feldhusen, J.; Grote, K.-H. *Pahl/Beitz Konstruktionslehre*; Springer: Berlin/Heidelberg, Germany, 2013; ISBN 978-3-642-29568-3.
6. Gümpel, P.; Gläser, S.; Jost, N.; Mertmann, M.; Seitz, N.; Strittmatter, J. *Formgedächtnislegierungen: Einsatzmöglichkeiten in Maschinenbau, Medizintechnik und Aktuatorik*; 2. Auflage; Expert Verlag: Renningen, Germany, 2018; ISBN 978-3-8169-2727-3.
7. Dimitris, C. *Lagoudas. Shape Memory Alloys*; Springer: Boston, MA, USA, 2008; ISBN 978-0-387-47684-1.
8. Sacco, E.; Lecce, L.; Auricchio, F.; Antonucci, V.; Concilio, A. *Shape Memory Alloy Engineering: For Aerospace, Structural, and Biomedical Applications*; Butterworth-Heinemann: Woburn, MA, USA, 2021; ISBN 978-0-12-819264-1.
9. Hornbogen, E.; Eggeler, G.; Werner, E. *Werkstoffe: Aufbau und Eigenschaften von Keramik-, Metall-, Polymer- und Verbundwerkstoffen*, 12th ed.; aktualisierte Auflage; Springer Vieweg: Berlin/Heidelberg, Germany, 2019; ISBN 9783662588468.
10. Elahinia, M.H. (Ed.) *Shape Memory Alloy Actuators*; John Wiley & Sons, Ltd.: Chichester, UK, 2015; ISBN 9781118426913.
11. Elahinia, M.H. *Shape Memory Alloy Actuators: Design, Fabrication, and Experimental Evaluation*; Wiley: Chichester, UK, 2016; ISBN 978-1-118-35944-0.
12. Kohl, M. *Entwicklung von Mikroaktoren aus Formgedächtnislegierungen*; Wissenschaftliche Bericht (FZKA 6718); Forschungszentrum Karlsruhe: Karlsruhe, Germany, 2002.
13. Huang, W. On the selection of shape memory alloys for actuators. *Mater. Des. 1980–2015* **2002**, *23*, 11–19. [CrossRef]
14. Hornbogen, E.; Warlimont, H.; Skrotzki, B. *Metalle: Struktur und Eigenschaften der Metalle und Legierungen*; Springer: Berlin/Heidelberg, Germany, 2019; ISBN 978-3-662-57762-2.
15. Treppmann, D. *Thermomechanische Behandlung von NiTi: (mit Lösungsansätzen für Qualitätssicherung und Normung von Formgedächtnislegierungen)*; Zugl.: Bochum, University, Dissertation, 1996, Als Ms. gedr; VDI-Verl.: Düsseldorf, Germany, 1997; ISBN 3183462052.

16. Renata, C.; Huang, W.M.; Le He, W.; Yang, J.J. Shape change/memory actuators based on shape memory materials. *J. Mech. Sci. Technol.* **2017**, *31*, 4863–4873. [CrossRef]
17. Akhras, G. Smart Materials and Smart Sytems for the future. *Can. Mil. J.* **2000**, *1*, 25–32.
18. Choi, S.-B. The Grand Challenges in Smart Materials Research. *Front. Mater.* **2014**, *1*, 11. [CrossRef]
19. Hornbogen; Schmitt. *Legierungen mit Formgedächtnis*; VS Verlag für Sozialwissenschaften: Wiesbaden, Germany, 1991; ISBN 3531083880.
20. Mohd Jani, J. Design Optimisation of Shape Memory Alloy Linear Actuator Applications. Ph.D. Thesis, RMIT University, Melbourne, Australia, 2016.
21. Kaack, M. Elastische Eigenschaften von NiTi-Formgedächtnis-Legierungen. Ph.D. Thesis, Ruhr-Universität Bochum, Bochum, Germany, 2002.
22. Lygin, K. *Eine Methodik zur Entwicklung von Umgebungsaktivierten FG-Aktoren Mit Geringer Thermischer Hysterese am Beispiel der Heizungs- und Klimatechnik*; Verlag Dr. Hut: München, Germany, 2014; ISBN 978-3-8439-1620-2.
23. Rehr, W. *Automatisierung mit Industrierobotern: Komponenten, Programmierung, Anwendung. Referate der Fachtagung Automatisierung mit Industrierobotern*; Rehr, W., Ed.; Vieweg+Teubner Verlag; Imprint: Wiesbaden, Germany, 1989; ISBN 9783663142249.
24. Bartenschlager, J.; Hebel, H.; Schmidt, G. *Handhabungstechnik mit Robotertechnik*; Vieweg+Teubner Verlag: Wiesbaden, Germany, 1998; ISBN 978-3-528-03830-4.
25. Bachl, W. *Qualifizierung an Industrierobotern*; Springer: Berlin/Heidelberg, Germany, 1986; ISBN 978-3-540-17018-1.
26. Feinmechanisches Fertigungszentrum Glashütte GmbH. Greiftechnik. Available online: https://ffz-glashuette.com/greiftechnik/ (accessed on 17 April 2024).
27. Scholtes, D.; Moske, M. Konstruktion Eines Festkörpergelenkgreifers mit Bistabiler Formgedächtnisaktorik 2021. Available online: https://www.researchgate.net/publication/352028703 (accessed on 16 October 2024).
28. Lu, Y.; Xie, Z.; Wang, J.; Yue, H.; Wu, M.; Liu, Y. A novel design of a parallel gripper actuated by a large-stroke shape memory alloy actuator. *Int. J. Mech. Sci.* **2019**, *159*, 74–80. [CrossRef]
29. Zhou, H.; Ma, N. Modeling and experimental implementation of a flexible SMA wire-based gripper for confined space operation. *J. Intell. Mater. Syst. Struct.* **2022**, *33*, 2161–2175. [CrossRef]
30. Rad, N.F.; Yousefi-Koma, A.; Rezaei, H.; Bazrafshani, M.A. Design and fabrication of a gripper actuated by shape memory alloy spring. In Proceedings of the 2016 4th International Conference on Robotics and Mechatronics (ICROM), Tehran, Iran, 26–28 October 2016; pp. 455–458, ISBN 978-1-5090-3222-8.
31. EPFL. Smart Grippers Powered by Shape Memory Alloys: Miniaturized Bistable SMA Gripper. Available online: https://www.epfl.ch/labs/lai/research/page-101809-en-html/page-153681-en-html/ (accessed on 17 April 2024).
32. Koh, J.-S. Design of Shape Memory Alloy Coil Spring Actuator for Improving Performance in Cyclic Actuation. *Materials* **2018**, *11*, 2324. [CrossRef] [PubMed]
33. Lee, J.-H.; Chung, Y.S.; Rodrigue, H. Long Shape Memory Alloy Tendon-based Soft Robotic Actuators and Implementation as a Soft Gripper. *Sci. Rep.* **2019**, *9*, 11251. [CrossRef] [PubMed]
34. Li, X.; Ma, Y.; Wu, C.; Wang, Y.; Zhou, S.; Gao, X.; Cao, C. A fast actuated soft gripper based on shape memory alloy wires. *Smart Mater. Struct.* **2024**, *33*, 45011. [CrossRef]
35. Motzki, P.; Seelecke, S.; Rizzello, G. A Shape Memory Alloy Smart Handling System for Advanced Manufacturing Applications. In Proceedings of the 2020 7th International Conference on Control, Decision and Information Technologies (CoDIT), Prague, Czech Republic, 29 January–2 July 2020; pp. 229–234, ISBN 978-1-7281-5953-9.
36. OnRobot A/S. 2FG7: Unkomplizierter Parallelgreifer für Beengte Platzverhältnisse und Anspruchsvolle Werkstücke. Available online: https://onrobot.com/de/produkte/2fg7 (accessed on 8 June 2024).
37. SCHUNK SE & Co. KG. PGL-plus-P: Universalgreifer. Available online: https://schunk.com/de/de/greiftechnik/parallelgreifer/pgl-plus-p/c/PGR_6511 (accessed on 8 June 2024).
38. Hamid, Q.Y.; Wan Hasan, W.Z.; Azmah Hanim, M.A.; Nuraini, A.A.; Hamidon, M.N.; Ramli, H.R. Shape memory alloys actuated upper limb devices: A review. *Sens. Actuators Rep.* **2023**, *5*, 100160. [CrossRef]
39. Miro, M.; Theren, B.; Schmelter, T.; Kuhlenkötter, B. SMA Actuator Usage in Upper Limb Rehabilitation Technology. In Proceedings of the ASME 2021 Conference on Smart Materials, Adaptive Structures and Intelligent Systems, Virtual, Online, 14–15 September 2021; American Society of Mechanical Engineers: Washington, DC, USA, 2021; p. 09142021, ISBN 978-0-7918-8549-9.
40. Deng, E.; Tadesse, Y. A Soft 3D-Printed Robotic Hand Actuated by Coiled SMA. *Actuators* **2021**, *10*, 6. [CrossRef]
41. Jeong, J.; Yasir, I.B.; Han, J.; Park, C.H.; Bok, S.-K.; Kyung, K.-U. Design of Shape Memory Alloy-Based Soft Wearable Robot for Assisting Wrist Motion. *Appl. Sci.* **2019**, *9*, 4025. [CrossRef]
42. Wang, Y.; Zheng, S.; Pang, J.; Li, S.; Li, J. Design and Experiment of a Hand Movement Device Driven by Shape Memory Alloy Wires. *J. Robot.* **2021**, *2021*, 1–13. [CrossRef]
43. Hadi, A.; Alipour, K.; Kazeminasab, S.; Elahinia, M. ASR glove: A wearable glove for hand assistance and rehabilitation using shape memory alloys. *J. Intell. Mater. Syst. Struct.* **2018**, *29*, 1575–1585. [CrossRef]
44. Taylor, F.; Au, C. Forced Air Cooling of Shape-Memory Alloy Actuators for a Prosthetic Hand. *J. Comput. Inf. Sci. Eng.* **2016**, *16*, 041004. [CrossRef]
45. Bishay, P.L.; Fontana, J.; Raquipiso, B.; Rodriguez, J.; Borreta, M.J.; Enos, B.; Gay, T.; Mauricio, K. Development of a biomimetic transradial prosthetic arm with shape memory alloy muscle wires. *Eng. Res. Express* **2020**, *2*, 35041. [CrossRef]

46. Simone, F.; Rizzello, G.; Seelecke, S.; Motzki, P. A Soft Five-Fingered Hand Actuated by Shape Memory Alloy Wires: Design, Manufacturing, and Evaluation. *Front. Robot. AI* **2020**, *7*, 608841. [CrossRef] [PubMed]
47. DYNALLOY, Inc. Technical Characteristics of FLEXINOL Actuator Wires. Available online: https://www.dynalloy.com/pdfs/TCF1140.pdf (accessed on 19 April 2024).
48. Rao, A.; Srinivasa, A.R.; Reddy, J.N. *Design of Shape Memory Alloy (SMA) Actuators*; Springer International Publishing: Cham, Switzerland, 2015; ISBN 978-3-319-03187-3.
49. Czechowicz, A.; Böttcher, J.; Mojrzisch, S.; Langbein, S. High Speed Shape Memory Alloy Activation. In *Volume 2: Mechanics and Behavior of Active Materials; Integrated System Design and Implementation; Bio-Inspired Materials and Systems; Energy Harvesting, Proceedings of the ASME 2012 Conference on Smart Materials, Adaptive Structures and Intelligent Systems, Stone Mountain, GA, USA, 19–21 September 2012*; American Society of Mechanical Engineers: Washington, DC, USA, 2012; pp. 451–454. ISBN 978-0-7918-4510-3.
50. Stephan, P.; Kabelac, S.; Kind, M.; Mewes, D.; Schaber, K.; Wetzel, T. *VDI-Wärmeatlas*; Springer: Berlin/Heidelberg, Germany, 2019; ISBN 978-3-662-52988-1.
51. Pelton, A.R.; Huang, G.H.; Moine, P.; Sinclair, R. Effects of thermal cycling on microstructure and properties in Nitinol. *Mater. Sci. Eng. A* **2012**, *532*, 130–138. [CrossRef]
52. Schmelter, T.; Theren, B.; Kielczewski, A.; Kuhlenkötter, B. Investigations of the Long-Term Behavior of Electrically Heated Shape Memory Alloy Wires Deflected by a 90° Pulley. In Proceedings of the ASME 2022 Conference on Smart Materials, Adaptive Structures and Intelligent Systems, Dearborn, MI, USA, 12–14 September 2022; American Society of Mechanical Engineers: Washington, DC, USA, 2022. ISBN 978-0-7918-8627-4.